

# Enhanced stability of dispersion-managed mode-locked fiber lasers with near-zero net cavity dispersion by high-contrast saturable absorbers

H. H. Liu and K. K. Chow\*

School of Electrical and Electronic Engineering, Nanyang Technological University, 50 Nanyang Avenue, Singapore 639798

\*Corresponding author: kkchow@ntu.edu.sg

Received Month X, XXXX; revised Month X, XXXX; accepted Month X, XXXX, posted Month X, XXXX (Doc. ID XXXXX); published Month X, XXXX

We experimentally investigate the stability of dispersion-managed mode-locked fiber lasers by using carbon-nanotube based saturable absorbers with different modulation depths. An unstable operation region of the mode-locked fiber laser with near-zero net cavity dispersion is observed where the laser produces random pulse burst rather than the stable pulse train. By the implementation of high-contrast saturable absorbers in the laser, the unstable region is found to be shrunk by  $\sim 31.3\%$  when the modulation depth of saturable absorbers increases from 6.4% to 12.5%. The numerical simulation is consistent with the experimental observation.

OCIS Codes: (060.3510) Lasers, fiber, (140.4050) Mode-locked lasers, (160.4330) Nonlinear optical materials.

Passively mode-locked fiber lasers have emerged as one of the best pulsed light sources for a broad range of applications including optical communication, frequency metrology, microscopy, and micromachining [1]. In particular, dispersion-managed mode-locked fiber lasers consist of anomalously or normally dispersive fibers present an attractive design to produce stretched pulses with excellent performance [2-4]. Previous reports have demonstrated that the best performance of output pulses in terms of large spectral bandwidth and low timing jitter can be achieved by managing the net cavity dispersion ( $\beta_{net}^{(2)}$ ) of the fiber laser approaching zero [5-8]. In a dispersion-managed mode-locked fiber laser, the spectral filtering induced by the limited gain bandwidth plays an important role as the spectrum broadens when  $\beta_{net}^{(2)}$  approaches zero which affects the laser stability [9]. Since the loss experienced by the pulse with a large spectral bandwidth is greater than that by continuum wave (CW) due to spectral filtering, CW could break through the pulse and causes instabilities [10]. Numerical studies have figured out that there is an unstable region in 1.55- $\mu\text{m}$  dispersion-managed mode-locked fiber lasers near zero  $\beta_{net}^{(2)}$  where stable output pulses cannot be obtained [11]. Such unstable region is also found in reported experimental works and limits the achievement of stable mode-locking with  $\beta_{net}^{(2)}$  towards zero [9, 12, 13]. In order to compensate such spectral filtering loss, one solution is to adopt saturable absorbers (SAs) with more absorption to CW than to high-intensity pulses in the laser cavities [10]. Theoretical studies have predicted that SAs with large modulation depth can assist fiber lasers to obtain stable mode-locking around zero  $\beta_{net}^{(2)}$  [14]. However, it is yet experimentally or numerically confirmed that how much of  $\beta_{net}^{(2)}$  can be pushed toward zero  $\beta_{net}^{(2)}$  for stable mode-locking by SAs with different modulation depths.

For the investigation of the influence of the SAs on mode-locked fiber lasers, semiconductor-based SA is one of the good candidates to obtain mode-locked fiber lasers with pre-defined modulation depth and stable operation [14-17]. Recently, it has shown that dispersion-managed

mode-locked fiber laser incorporating carbon-nanotube based SAs (CNT-SAs) can generate pulses with a pulse width of  $\sim 74$  fs and a spectral bandwidth of  $\sim 63$  nm when  $\beta_{net}^{(2)}$  is  $-0.003$  ps<sup>2</sup> [18]. In this Letter, we experimentally investigate the stability of dispersion-managed mode-locked fiber laser with  $\beta_{net}^{(2)}$  near zero by using CNT-SAs with different modulation depths. Experimental results show that the unstable region of the laser could be shrunk by  $\sim 31.3\%$  when the modulation depth of SA increases from 6.4% to 12.5%. The numerical analysis is also performed to investigate the dispersion-managed mode-locked fiber laser with different modulation depths of SAs, which is consistent with the experimental observation. The obtained results are not merely applicable to the dispersion-managed mode-locked fiber laser incorporating CNT-SAs, but also could be a general guidance for the laser using similar kinds of SAs.

Figure 1 shows the experimental setup of the dispersion-managed mode-locked fiber laser incorporating CNT-SAs. The 7.32-m-long erbium-doped fiber (EDF) with the group velocity dispersion parameter ( $\beta^{(2)}$ ) of  $+23.4$  ps<sup>2</sup>/km is pumped by a 976-nm pump laser via a 980/1550-nm wavelength division multiplexing (WDM)

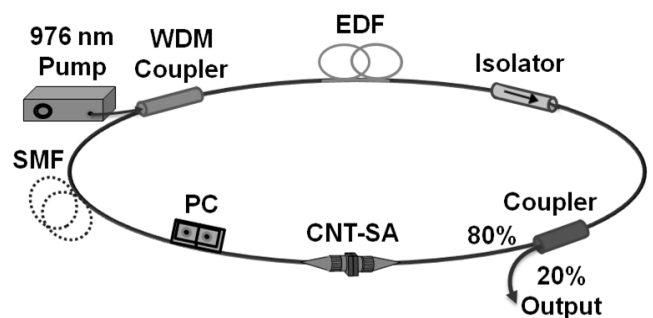


Fig. 1. Experimental setup of dispersion-managed mode-locked fiber laser incorporating carbon-nanotube-based saturable absorber (CNT-SA). WDM coupler: wavelength division multiplexing coupler; EDF: erbium-doped fiber; PC: polarization controller; SMF: single-mode fiber.

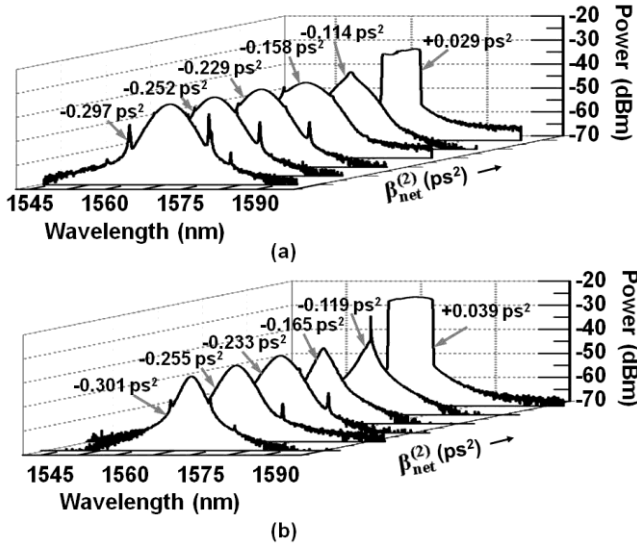


Fig. 2. Experimental results of the output spectra of the dispersion-managed mode-locked fiber lasers with different net cavity dispersion using CNT-SAs with modulation depths of (a) 12.5% and (b) 6.4%.

coupler. The EDF has a mode-field diameter of  $\sim 5.9 \mu\text{m}$  and a peak absorption of  $\sim 6 \text{ dB/m}$  at  $1530 \text{ nm}$ . The WDM coupler comes with a  $0.66\text{-m}$ -long HI1060 fiber pigtail with  $\beta^{(2)}$  of  $+20 \text{ ps}^2/\text{km}$ . A polarization-insensitive optical isolator is applied to ensure unidirectional propagation of the light in the cavity. The 80/20 coupler extracts 20% of optical power from the laser cavity as the laser output. A fiber-based polarization controller (PC) is included for optimizing the mode-locking condition. The CNT-SA is constructed by connecting two fixed connection/physical contact (FC/PC) connector ends, in which one of the connector ends is deposited with CNTs by optically-driven deposition method [19]. The CNTs are prepared by a bulk production method called high-pressure CO conversion (HiPCO) and well dispersed in dimethylformamide (DMF) solvent through the purification process [20]. Two CNT-SAs with modulation depths of 12.5% and 6.4% are employed in this work, exhibiting non-saturable losses of 47% and 28.1%, respectively.  $\beta_{net}^{(2)}$  is changed ranging from  $-0.31$  to  $+0.04 \text{ ps}^2$  by shortening the length of standard single mode fiber (SMF) in the laser cavity.

Figure 2(a) shows the measured spectra of the developed fiber laser incorporating the CNT-SA with

modulation depth of 12.5%. When the laser operates with net anomalous dispersion ( $\beta_{net}^{(2)} = -0.297 \text{ ps}^2$ ), the self-started mode-locking can be achieved at a relatively low pump power of  $\sim 4 \text{ mW}$ . The strong Kelly-sidebands are superimposed on the spectrum, which indicates that the laser operates in the conventional soliton regime [21]. The single pulse generation is confirmed by the corresponding RF spectrum as well as the autocorrelation trace. Such laser produces pulses with the pulse width of  $\sim 640 \text{ fs}$ , the spectral bandwidth of  $\sim 4.9 \text{ nm}$ , and the single-pulse energy of  $\sim 14 \text{ pJ}$ . When the relative amount of negative to positive dispersion fiber is reduced by shortening the length of SMF ( $\beta_{net}^{(2)} = -0.158 \text{ ps}^2$ ), the Kelly-sidebands are found to gradually move away from the center wavelength

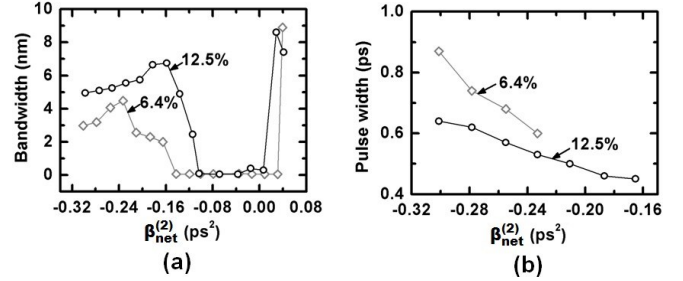


Fig. 3. Plots of output (a) spectral bandwidth and (b) pulse width against net cavity dispersion of dispersion-managed mode-locked fiber lasers using CNT-SAs with different modulation depths.

while the spectrum turns into a Gaussian-like shape associated with spectrum broadening. The relatively clean spectrum indicates that the laser transits into the dispersion-managed soliton regime (or stretched-pulse) [2]. The laser produces pulses with the pulse width of  $\sim 450 \text{ fs}$ , the spectral bandwidth of  $\sim 6.8 \text{ nm}$ , and the single-pulse energy of  $\sim 11.2 \text{ pJ}$  under the pump power of  $\sim 4 \text{ mW}$ . By further increasing  $\beta_{net}^{(2)}$  to  $-0.114 \text{ ps}^2$ , the spectrum changes to a nearly triangular shape showing a weak CW spike on the center wavelength. Under this condition, the laser only produces the random pulse burst rather than the stable pulse train no matter how the pump power and the state of polarization controller are adjusted. When  $\beta_{net}^{(2)}$  is increased to be normal dispersion ( $\beta_{net}^{(2)} = +0.029 \text{ ps}^2$ ), the spectrum with a rectangular shape can be observed by adjusting the polarization controller under the pump power of  $\sim 17 \text{ mW}$ . The laser generates pulses with the pulse width of  $\sim 50 \text{ ps}$ , the spectral bandwidth of  $\sim 8.6 \text{ nm}$ , and the single-pulse energy of  $\sim 86 \text{ pJ}$ . The pulse width can be further compressed outside the laser cavity to  $\sim 870 \text{ fs}$  using SMF with an optimized length of  $\sim 536 \text{ m}$ . The steep edges of spectrum and the highly-chirped pulse imply that the mode-locked fiber laser operates in the dissipative soliton regime [22].

For comparison, the experiment is repeated using the same fiber laser incorporating the CNT-SA with modulation depth of 6.4% as shown in Fig. 2(b). The operation of laser transits from the conventional soliton with relatively large net anomalous dispersion ( $\beta_{net}^{(2)} = -0.301 \text{ ps}^2$ ) into the dissipative soliton with net normal dispersion ( $\beta_{net}^{(2)} = +0.039 \text{ ps}^2$ ), while tends to be unstable with  $\beta_{net}^{(2)}$  approaching zero ( $\beta_{net}^{(2)} = -0.165 \text{ ps}^2$ ).

Figure 3(a) plots the spectral bandwidth against net cavity dispersion for the lasers with two different CNT-SAs. When the absolute value of  $\beta_{net}^{(2)}$  is close to zero, the spectral bandwidth gradually increases and then sharply decreases. The significant decrease in the spectral bandwidth is a reflection of the unstable operation of laser. For the fiber laser incorporating the CNT-SA with modulation depth of 6.4%, the unstable region is found to be in the range of  $-0.233 \text{ ps}^2 < \beta_{net}^{(2)} < +0.039 \text{ ps}^2$ . On the other hand, for the case of CNT-SA with modulation depth of 12.5%, the unstable region of the laser is measured in the range of  $-0.158 \text{ ps}^2 < \beta_{net}^{(2)} < +0.029 \text{ ps}^2$ . The results show that the unstable region in the dispersion-managed mode-locked fiber laser could be

shrunk by  $\sim 31.3\%$  when the modulation depth of SAs increases from 6.4% to 12.5%. Figure 3(b) shows the pulse width versus  $\beta_{net}^{(2)}$  in net anomalous dispersion region. The pulse width decreases as  $\beta_{net}^{(2)}$  approaches zero. The shortest pulse width is obtained around 450 fs with  $\beta_{net}^{(2)}$  of  $-0.158 \text{ ps}^2$  when the CNT-SA with modulation depth of 12.5% is applied.

Numerical simulation is performed to qualitatively analyze the role of SAs in dispersion-managed mode-locked fiber lasers. The numerical model is similar to the experimental setup as shown in Fig. 1. A piece of gain fiber is connected to a HI1060 fiber. The length of SMF after the SA is adjusted to manage  $\beta_{net}^{(2)}$ . Light propagation within each fiber section can be modeled by the modified nonlinear Schrödinger equation (NLSE) [23]:

$$\frac{\partial A(\xi, T)}{\partial \xi} + \frac{i}{2}(\beta^{(2)} + ig \frac{1}{\Omega_g}) \frac{\partial^2 A(\xi, T)}{\partial T^2} = \gamma |A(\xi, T)|^2 A(\xi, T) + \frac{g}{2} A(\xi, T) \quad (1)$$

where  $A(\xi, T)$  is the envelope of the field,  $\xi$  is the propagation coordinate,  $T$  is the time scaled to the pulse duration,  $\beta^{(2)}$  is the group velocity dispersion parameter,  $\gamma$  is the nonlinear parameter, and  $\Omega_g$  is the gain bandwidth. The gain  $g$  is given by:

$$g = g_0 \left[ 1 + P_{ave} / P_{sat} \right] \quad (2)$$

where  $g_0$  is the small signal gain,  $P_{sat}$  is the gain saturation power, and  $P_{ave}$  is the average power of the pulse train. The intensity-dependent transmittance  $T(I)$  of the SA is expressed by:

$$T(I) = 1 - (a_0 \left[ 1 + I / I_{sat} \right] + a_{ns}) \quad (3)$$

where  $I$  is the instantaneous intensity of the pulse,  $I_{sat}$  is the saturation intensity of SA,  $a_{ns}$  refers to the non-saturable loss, and  $a_0$  is the modulation depth which also accounts for transmission contrast of SAs. Provided that  $L$  refers to the fiber length and  $i$  denotes each fiber section, the net cavity dispersion  $\beta_{net}^{(2)}$  can be given by:

$$\beta_{net}^{(2)} = \sum_i L_i \times \beta_i^{(2)} \quad (4)$$

Fiber type	$\beta^{(2)}$ (ps <sup>2</sup> /km)	$\gamma$ (W <sup>-1</sup> km <sup>-1</sup> )	L(m)	$g_0$	$P_{sat}$ (mW)
EDF	+23.4	2.69	7.32	2	5
HI1060	+20	1.5	0.66	0	0
SMF	-22	1.06	Var.	0	0

EDF: erbium-doped fiber; SMF: single-mode fiber; Var.: variable.

The cavity parameters used in the simulation are summarized in Table 1. The gain bandwidth is  $\Omega_g = 5.5$  THz. In order to investigate specifically the influence of the modulation depth on the stability of dispersion-managed mode-locked fiber lasers, only  $a_0$  and  $L_{SMF}$  are changed while the other parameters are kept constant.  $I_{sat}$  is set to be 10 MW/cm<sup>2</sup> referring to the typical value of CNT-based SAs [24].  $a_{ns}$  is assumed to be 15% corresponding to the minimum non-saturable loss of CNT-SA with a desirable modulation depth obtained in our experiments [19]. The numerical model is solved with a standard split-step Fourier algorithm.

Figure 4 shows the numerical results about the laser with  $a_0 = 12.5\%$  at different  $\beta_{net}^{(2)}$ . For  $\beta_{net}^{(2)} = -0.172 \text{ ps}^2$ ,

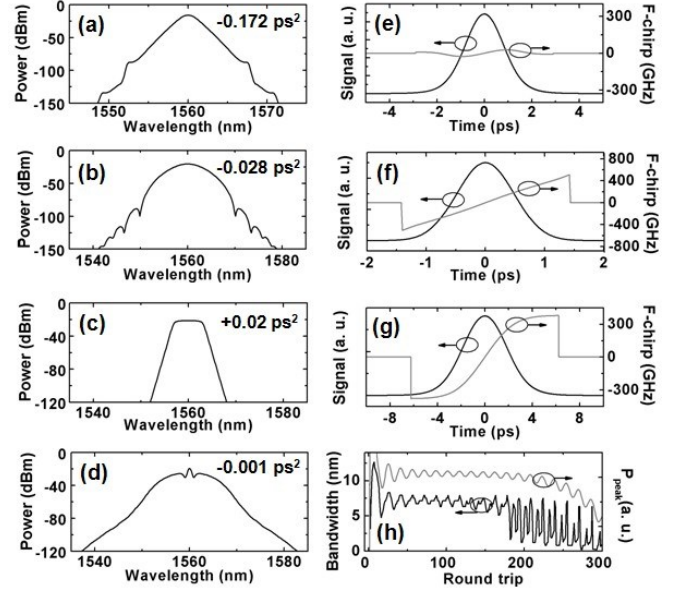


Fig. 4. Numerical results of output spectra of dispersion-managed mode-locked fiber lasers with net cavity dispersion of (a)  $-0.172 \text{ ps}^2$ , (b)  $-0.028 \text{ ps}^2$ , and (c)  $+0.02 \text{ ps}^2$ ; (e), (f) and (g) are the corresponding temporal pulses showing together with the frequency-chirps; (d) is the output spectrum of the laser with net cavity dispersion of  $-0.001 \text{ ps}^2$ , and (h) is the evolution of the spectral bandwidth and the peak power against the number of round trip in the cavity.

the Kelly-sidebands are superimposed on the spectrum as shown in Fig. 4(a), which could be explained by the periodic perturbations such as gain, filtering and loss [21]. Figure 4(e) shows the corresponding pulse fitted by a sech<sup>2</sup>-profile, which exhibits a negligible frequency-chirp across the duration. Such chirp-free pulse is a result of the phase-cancellation between the anomalous dispersion and the self-phase modulation. For  $\beta_{net}^{(2)} = -0.028 \text{ ps}^2$ , the spectrum exhibits a wide spectral bandwidth as illustrated in Fig. 4(b). The corresponding pulse shows a

linear frequency-chirp as given in Fig. 4(f). The up-chirp is due to the output after the normal dispersion gain fiber. Further increasing  $\beta^{(2)}$  to  $+0.02 \text{ ps}^2$ , the output spectrum with steep edges can be observed as shown in Fig. 4(c). The corresponding pulse is highly chirped with a relatively wide pulse width as plotted in Fig. 4(g), confirming that the laser operates in the dissipative soliton regime.

Figure 4(d) simulates the spectrum of the laser with  $\beta_{net}^{(2)}$  of  $-0.001 \text{ ps}^2$ . A small CW spike is superimposed on the center wavelength of the spectrum, while no stable pulse can be maintained in time-domain. Although it is difficult to estimate precisely the parameters from the real laser cavity, one can find the general agreement with the experimental observation. Figure 4(h) plots the evolution of the spectral bandwidth and the peak power of the pulse against cavity round trip. In the beginning, the initial pulse from the amplified spontaneous emission (ASE) noise is reshaped by the SA, and followed by amplification via gain fiber, which enhances the peak power of pulse. Subsequently, the spectrum broadens due to self-phase modulation. As the spectral bandwidth gets

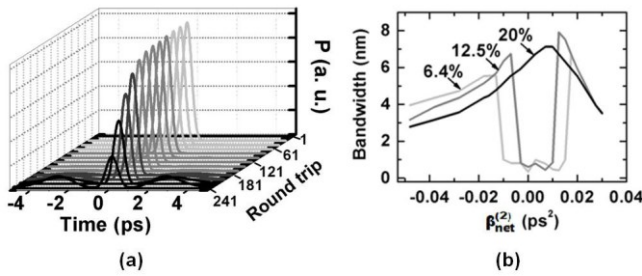


Fig. 5. (a) Plot of temporal pulse evolution against the number of round trip in the laser when net cavity dispersion is  $-0.001 \text{ ps}^2$ ; and (b) the spectral bandwidth against net cavity dispersion for the lasers incorporating different saturable absorbers with modulation depths of 6.4%, 12.5%, and 20%.

wider, the spectral filtering due to the finite gain bandwidth plays an increasingly important role that in turn increases the loss experienced by the pulses. When the loss deviates substantially and cannot be caught up by the cavity gain, the peak power of pulse is correspondingly decreased. As a result, the weak nonlinear effect is insufficient to support the broadband mode-locking and the instabilities grow.

Figure 5(a) shows the pulse evolution in the laser with  $\beta_{net}^{(2)}$  of  $-0.001 \text{ ps}^2$ . The initial seed is an arbitrary weak pulse. After hundreds of cavity round trips, the built-up pulse is gradually shed away. In order to reshape the pulse to achieve a desirable peak power, a SA with large modulation depth is necessary. Figure 5(b) shows the spectral bandwidth against  $\beta_{net}^{(2)}$  for the lasers with different modulation depths of SAs. The unstable region of the laser can be shrunk by  $\sim 36\%$  when  $a_0$  is changed from 6.4% to 12.5%. In the case of a SA with  $a_0$  of 20%, the laser can operate in a stable mode-locking state across the entire dispersion region. It is observed that for a large  $a_0$ , the spectral bandwidth tends to decrease near zero  $\beta_{net}^{(2)}$ . It implies that the residual saturable absorption could contribute to the cavity loss, which might decrease the threshold for Q-switching instability [25]. In order to obtain laser mode-locking with minimum unstable region,  $a_0$  is optimized at 16% for the given cavity parameters. Since the same  $\beta_{net}^{(2)}$  can be designed by various combinations of fibers, we also numerically analysis the dispersion-managed mode-locked fiber laser with a short-length cavity. The relationship between the spectral bandwidth and  $\beta_{net}^{(2)}$  for the laser with different  $a_0$  shows the similar trend to Fig. 5(b). Note that the unstable region of the fiber laser with  $a_0 = 12.5\%$  can also be minimized by setting the gain bandwidth to 12.5 THz. This further verifies that the origin of the instabilities is related to the strong spectral filtering.

In conclusion, we investigate the stability of dispersion-managed mode-locked fiber laser with net cavity dispersion near zero by using carbon-nanotube based saturable absorbers with different modulation depths. Experimental results demonstrate that the unstable region of the dispersion-managed mode-locked fiber laser can be reduced by  $\sim 31.3\%$  when the modulation depth of SAs increases from 6.4% to 12.5%. The SA with a large modulation depth can assist laser cavity to stabilize the mode-locking operation. The simulated result is consistent with the experimental observation, which can be a

general guidance for the similar dispersion-managed mode-locked fiber laser system. Acknowledgements

This work was partially supported by Academic Research Fund Tier 1 Grant (RG22/10) of Ministry of Education (MOE) and NTU, Singapore.

## References

1. M. E. Fermann and I. Hartl, *IEEE J. Sel. Topics Quantum Electron.* 15, 191 (2009).
2. H. A. Haus, K. Tamura, L. E. Nelson, E. P. Ippen, *IEEE J. Quantum Electron.* 31, 591 (1995).
3. D. Y. Tang and L. M. Zhao, *Opt. Lett.* 32, 41 (2007).
4. F. Ö. Ilday, F. W. Wise, and T. Sosnowski, *Opt. Lett.* 27, 1531 (2002).
5. D. Ma, Y. Cai, C. Zhou, W. Zong, L. Chen, and Z. Zhang, *Opt. Lett.* 35, 2858 (2010).
6. L. Nugent-Glandorf, T. A. Johnson, Y. Kobayashi, and S. A. Diddams, *Opt. Lett.* 36, 1578 (2011).
7. Y. Song, K. Jung, and J. Kim, *Opt. Lett.* 36, 1761 (2011).
8. Y. Song, C. Kim, K. Jung, H. Kim, and J. Kim, *Opt. Express* 19, 14518 (2011).
9. K. Kieu and F. W. Wise, in *Conference on Lasers and Electro-Optics/International Quantum Electronics Conference*, OSA Technical Digest (CD) (Optical Society of America, 2009), p. CML3.
10. F. X. Kärtner, J. A. der Au and U. Keller, *IEEE J. Quantum Electron.* 4, 159 (1998).
11. S. Chouli, J. M. Soto-Crespo, and P. Grelu, *Opt. Express* 19, 2959 (2011).
12. N. Nishizawa, Y. Nozaki, E. Itoga, H. Kataura, and Y. Sakakibara, *Opt. Express* 19, 21874 (2011).
13. Y. Nozaki, N. Nishizawa, E. Omoda, H. Kataura, and Y. Sakakibara, *Opt. Lett.* 37, 5079 (2012).
14. R. Herda and O. G. Okhotnikov, *IEEE J. Quantum Electron.* 40, 893 (2004).
15. S. Yamashita, *J. Lightw. Technol.* 30, 427 (2012).
16. J. Lim, K. Knabe, K. A. Tillman, W. Neely, Y. Wang, R. A. Correa, F. Couny, P. S. Light, F. Benabid, J. C. Knight, K. L. Corwin, J. W. Nicholson, and B. R. Washburn, *Opt. Express* 17, 14115 (2009).
17. M. Zhang, E. J. R. Kelleher, A. S. Pozharov, E. D. Obraztsova, S. V. Popov, and J. R. Taylor, *Opt. Lett.* 36, 3984 (2011).
18. D. Popa, Z. Sun, T. Hasan, W. B. Cho, F. Wang, F. Torrisi, and A. C. Ferrari, *Appl. Phys. Lett.* 101, 153107 (2012).
19. H. H. Liu, Y. Yang and K. K. Chow, *Opt. Express* 21, 18975 (2013).
20. K. K. Chow, S. Yamashita, and S. Y. Set, *Opt. Lett.* 35, 2070 (2010).
21. L. E. Nelson, D. J. Jones, K. Tamura, H. A. Haus, and E. P. Ippen, *Appl. Phys. B* 65, 277 (1997).
22. P. Grelu, and N. Akhmediev, *Nature Photon.* 6, 84 (2012).
23. G. P. Agrawal, *Nonlinear fiber optics*, 4rd ed. (Academic 2009).
24. S. Y. Set, H. Yaguchi, Y. Tanaka, and M. Jablonski, *J. Select. Top. Quantum Electron.* 10, 137 (2004).
25. C. Hönninger, R. Paschotta, F. Morier-Genoud, M. Moser, and U. Keller, *J. Opt. Soc. Am. B* 16, 46 (1999).

## Full References

1. M. E. Fermann and I. Hartl, 'Ultrafast fiber laser technology', *IEEE J. Sel. Topics Quantum Electron.* 15, 191 (2009).
2. H. A. Haus, K. Tamura, L. E. Nelson, E. P. Ippen, 'Stretched-pulse additive pulse mode-locking in fiber ring lasers: theory and experiment', *IEEE J. Quantum Electron.* 31, 591 (1995).
3. D. Y. Tang and L. M. Zhao, 'Generation of 47-fs pulses directly from an erbium-doped fiber laser', *Opt. Lett.* 32, 41 (2007).
4. F. Ö. Ilday, F. W. Wise, and T. Sosnowski, 'High-energy femtosecond stretched-pulse fiber laser with a nonlinear optical loop mirror', *Opt. Lett.* 27, 1531 (2002).
5. D. Ma, Y. Cai, C. Zhou, W. Zong, L. Chen, and Z. Zhang, '37.4 fs pulse generation in an Er: fiber laser at a 225 MHz repetition rate', *Opt. Lett.* 35, 2858 (2010).
6. L. Nugent-Glandorf, T. A. Johnson, Y. Kobayashi, and S. A. Diddams, 'Impact of dispersion on amplitude and frequency noise in a Yb-fiber laser comb', *Opt. Lett.* 36, 1578 (2011).
7. Y. Song, K. Jung, and J. Kim, 'Impact of pulse dynamics on timing jitter in mode-locked fiber lasers', *Opt. Lett.* 36, 1761 (2011).
8. Y. Song, C. Kim, K. Jung, H. Kim, and J. Kim, 'Timing jitter optimization of mode-locked Yb-fiber lasers toward the attosecond regime', *Opt. Express* 19, 14518 (2011).
9. K. Kieu and F. W. Wise, 'Self-similar and stretched-pulse operation of erbium-doped fiber lasers with carbon nanotubes saturable absorber', in *Conference on Lasers and Electro-Optics/International Quantum Electronics Conference*, OSA Technical Digest (CD) (Optical Society of America, 2009), p. CML3.
10. F. X. Kärtner, J. A. der Au and U. Keller, 'Mode-locking with slow and fast saturable absorbers-what's the difference?', *IEEE J. Quantum Electron.* 4, 159 (1998).
11. S. Chouli, J. M. Soto-Crespo, and P. Grelu, 'Optical spectra beyond the amplifier bandwidth limitation in dispersion-managed mode-locked fiber lasers', *Opt. Express* 19, 2959 (2011).
12. N. Nishizawa, Y. Nozaki, E. Itoga, H. Kataura, and Y. Sakakibara, 'Dispersion-managed, high-power, Er-doped ultrashort-pulse fiber laser using carbon-nanotube polyimide film', *Opt. Express* 19, 21874 (2011).
13. Y. Nozaki, N. Nishizawa, E. Omoda, H. Kataura, and Y. Sakakibara, 'Power scaling of dispersion-managed Er-doped ultrashort pulse fiber laser with single wall carbon nanotubes', *Opt. Lett.* 37, 5079 (2012).
14. R. Herda and O. G. Okhotnikov, 'Dispersion compensation-free fiber laser mode-locked and stabilized by high-contrast saturable absorber mirror', *IEEE J. Quantum Electron.* 40, 893 (2004).
15. S. Yamashita, 'A Tutorial on Nonlinear Photonic Applications of Carbon Nanotube and Graphene', *J. Lightw. Technol.* 30, 427 (2012).
16. J. Lim, K. Knabe, K. A. Tillman, W. Neely, Y. Wang, R. A. Correa, F. Couny, P. S. Light, F. Benabid, J. C. Knight, K. L. Corwin, J. W. Nicholson, and B. R. Washburn, 'A phase-stabilized carbon nanotube fiber laser frequency comb', *Opt. Express* 17, 14115 (2009).
17. M. Zhang, E. J. R. Kelleher, A. S. Pozharov, E. D. Obraztsova, S. V. Popov, and J. R. Taylor, 'Passive synchronization of all-fiber lasers through a common saturable absorber', *Opt. Lett.* 36, 3984 (2011).
18. D. Popa, Z. Sun, T. Hasan, W. B. Cho, F. Wang, F. Torrisi, and A. C. Ferrari, '74-fs nanotube-mode-locked fiber laser', *Appl. Phys. Lett.* 101, 153107 (2012).
19. H. H. Liu, Y. Yang and K. K. Chow, 'Enhancement of thermal damage threshold of carbon-nanotube-based saturable absorber by evanescent-field interaction on fiber end', *Opt. Express* 21, 18975 (2013).
20. K. K. Chow, S. Yamashita, and S. Y. Set, 'Four-wave mixing based wavelength conversion using a single-walled carbon-nanotube-deposited planar lightwave circuit waveguide', *Opt. Lett.* 35, 2070 (2010).
21. L. E. Nelson, D. J. Jones, K. Tamura, H. A. Haus, and E. P. Ippen, 'Ultrashort-pulse fiber ring lasers', *Appl. Phys. B* 65, 277 (1997).
22. P. Grelu, and N. Akhmediev, 'Dissipative solitons for mode-locked lasers', *Nature Photon.* 6, 84 (2012).
23. G. P. Agrawal, *Nonlinear fiber optics*, 4rd ed. (Academic 2009).
24. S. Y. Set, H. Yaguchi, Y. Tanaka, and M. Jablonski, "Ultrafast fiber pulsed lasers incorporating carbon nanotubes," *J Select. Top. Quantum Electron.* 10, 137 (2004).
25. C. Hönniger, R. Paschotta, F. Morier-Genoud, M. Moser, and U. Keller, 'Q-switching stability limits of continuous-wave passive mode locking', *J. Opt. Soc. Am. B* 16, 46 (1999).